ACS OMEGA

http://pubs.acs.org/journal/acsodf

Article

Ambient-Dried, Ultra-high Strength, Low Thermal Conductivity, High Char Residual Rate F-type Polybenzoxazine Aerogel

Guoqiang Qin, Shilun Jiang, Haotian Zhang, Shengjian Qin, Hongya Wu, Feipeng Zhang, and Guanglei Zhang*

Cite This: *ACS Omega* 2022, 7, 26116−26122

Read Online

ACCESS | Metrics & More | Article Recommendations

ABSTRACT: The effect of the curing temperature (T_c) on the properties of PBO aerogel was investigated in this paper. The compressive strength of PBO aerogel prepared was much higher than that of PBO aerogel of the same density in other kinds of literature. With the robust F-type polybenzoxazine (PBO) aerogels with ultra-high Young's modulus (733.7 MPa at 0.48 g/cm^3 and 1070 MPa at 0.57 g/cm^3), excellent properties were obtained through a facile and scalable room-temperature HCl-catalyzed sol−gel method, followed by the ambient pressure drying technique. It is found that T_c plays a vital role in the polymerization process and the evolution of the microstructure of the 3D porous PBO network, where the necks between the nanoparticles become thick and strong when T_c is up to 150 °C, resulting in a pearl necklace-to-worm transformation in the micro-structure and significant growth in mechanical properties, but if T_c is higher than 180 °C, the pore volume and specific surface area will decrease sharply. Moreover, all synthetic PBO aerogels here possessed inherent flame retardancy and a high residual char rate in the volume density (0.32−0.57 g/cm^3). These properties make the F-type PBO aerogels a candidate material in aerospace applications or other fields.

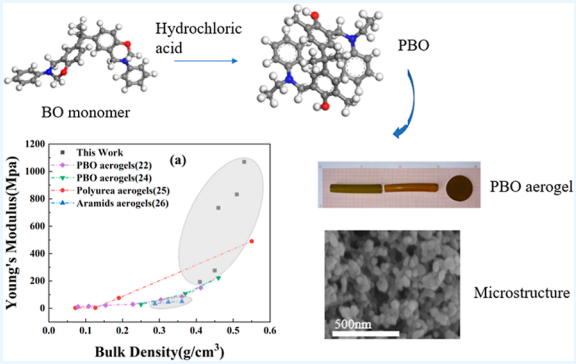

1. INTRODUCTION

Aerogel is a solid material assembled from nanoparticles with a three-dimensional structure and ultra-high porosity, extremely low density, high density, and specific surface area.[1,2] Aerogels were first made by Kistler[3] in the 1930s. After years of development, the types of aerogels have been diversified, and their applications based on low refractive index, high porosity, low density, and large surface area in many fields such as heat insulation, sound insulation, catalysis, filtration, and lightweight structural materials have attracted increasing attention all over the world. However, unfortunately, the mechanical properties of most current organic or inorganic aerogels are unacceptable. They are often too soft or fragile to act as monophase materials, just like the typical case of silica aerogel.[4,5] On the other hand, the preparation of high-performance aerogels requires some extraordinary or very harsh conditions [normally supercritical, a supercritical fluid (SCF) drying] to prevent the micropore structure from being destroyed in the drying process. These preparation technologies significantly improve the complexity or difficulty of preparing aerogels and often become bottlenecks, which not only enhance the cost and time consumption but also significantly hamper the large-scale production and promotion of aerogels. Therefore, the robust aerogel that can be prepared under conventional preparation conditions is urgently needed.

The emergence of the benzoxazine (BO) polymer and polybenzoxazine (PBO) aerogels are expected to provide effective solutions for the problems mentioned above. The PBO polymer, first produced by Holly and Cope[6] through the Mannich reaction in 1944, is a thermosetting phenolic resin containing N, O, and six chief oxazine ring structures. This material has many superior properties, such as excellent dynamic and static mechanical properties, high heat stability, high residual char rate, flame retardancy, almost zero shrinkage during the curing process, no small molecule release during production to pollute the environment,[7−10] and cheapness in price. Therefore, PBO is an ideal material for preparing high-strength flame-retardant aerogel.[11−13]

The aerogel prepared from PBO will be naturally hydrophobic and has high thermal stability. In addition, because PBO is a thermosetting resin, the strength of PBO aerogel can be controlled by controlling the heat treatment temperature. The currently prepared PBO aerogels are often used as

Received: March 4, 2022
Accepted: July 6, 2022
Published: July 18, 2022

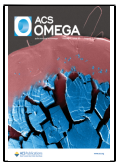

precursors for the preparation of char aerogels.[14] They are also used in thermal insulation, adsorption, supercapacitors, medical hard tissue scaffolds, catalyst carriers, and other fields.[15−19]

There have been some studies dedicated to the synthesis and preparation of PBO aerogels. Lorraine[18] first dissolved bisphenol A/aniline BO in xylene. Then, the partially cured PBO gel was placed at 130 °C for 96 h, followed by drying at room temperature and pressure for 2 days to get rid of xylene, to get organic aerogel and then heated and cured to get PBO aerogel with a density of 0.26~0.59 g/cm^3. After that, Shruti[20] and Xiao[21] performed a high-yield room-temperature acid-catalyzed synthesis method with hydrochloric acid employed to achieve ring-opening polymerization of PBO aerogels. As a result, the thermal catalytic-polymerization time was shortened from several days to several hours. Meanwhile, the HCl-catalyzed process engaged the para position of the aniline moieties, leading to a higher degree of cross-linking, but SCF CO_2 was also needed in their methods. The compressive strength of the obtained aerogel reached 14.42 MPa.[21]

To get rid of the restriction of SCF drying, some attempts have been made. Sadeq and co-authors[23] used acid-catalyzed ring-opening polymerization and the atmospheric pressure drying method. They successfully achieved PBO aerogels with inherent flame-retardant properties, hydrophobicity, and excellent mechanical properties. Typically, the obtained PBO aerogels are mechanically strong with strength (e.g., 1 MPa at 0.24 g/cm^3 at room temperature) and Young's modulus E (222.38 ± 6.63 MPa) higher than those of other high-performance aerogels of similar density, including polyimide and polyamide (Kevlar-like) aerogels, as well as polymer cross-linked X-silica and X-vanadia aerogels, at a significantly lower cost. Xiao[22] also prepared PBO aerogel using the bisphenol A-type BO monomer as a raw material and drying at atmospheric pressure. Despite the remarkable progress mentioned above, however, high-strength multifunctional aerogels through a convenient and straightforward method are still one of the research pursuits.

In this paper, we explore the influence of different curing temperatures on the properties of PBO aerogel and use a new BO monomer to prepare PBO aerogel with excellent strength. In this paper, robust F-type PBO aerogels with ultra-high Young's modulus is reported. It can be conveniently prepared by simply amplifying acid catalysis and the atmospheric drying process. Typically, bisphenol F, instead of traditional bisphenol A, is used as the precursor for polymerization. The prepared PBO aerogel possesses a distinct three-dimensional disordered nanopore network in a wide range of densities and excellent properties, such as ultra-high Young's modulus, high specific surface area, high residual char rate, high thermal stability, flame retardation, and hydrophobicity. These unique properties make it have excellent application prospects in thermal insulation, adsorption, supercapacitors, medical hard tissue scaffolds, catalyst carriers, or act as char aerogel precursors.

2. CHARACTERIZATION OF POLYBENZOXAZINE AEROGEL

The micromorphology of PBO aerogel samples was analyzed by using the HITACHI MC1000 microscope under 10 KV acceleration voltage. The material was ground into a fine powder before the test. Since PBO aerogel had no electrical conductivity, gold spraying was carried out before SEM analysis. The thermal stability of PBO aerogel was analyzed by using the TG209 F3 thermogravimetric analyzer at a temperature range of 100−900 °C and at an Ar rate of 90 mL/min, using a sample size of 5 mg.

The infrared spectrum of PBO aerogel was obtained by using the Thermo Fisher IS50 FTIR analyzer, and the wavenumber range was 400−4000 cm^{-1}. The sample was sliced and polished on both sides.

The thermal conductivity of aerogel was measured by using the DRX−II−RW type thin-film thermophysical tester. The thermophysical tester adopted an advanced transient heat flow method and longitudinal heat flow technology, and the thermal conductivity coefficient was calculated between 0.015 and 100 W/MK. The tested samples were of regular shape and had a diameter of 30 mm and thickness of 0.02−20 mm. The temperature range is between room temperature and 200 °C.

The TIAN CHEN WDW-100 universal testing machine was used to test the mechanical properties of samples, mainly for the compression test of aerogel at room temperature and pressure. The columnar aerogel samples with shape rules of φ = 5 mm and H = 20 mm were selected for the test, and 3 of each piece were selected for the test, and the test results were averaged. The loading speed was 0.1 mm/s, the maximum pressure before fracture was measured, and the compressive strength of the sample was calculated.

3. EXPERIMENTAL SECTION

The BO monomer was purchased from Chengdu Keyi Polymer Co., Ltd(China). *N*,*N*-dimethylformamide (DMF, AR) solvent was purchased from Tian Jin Fuyu Fine Chemical Co, Ltd. Acetonitrile was purchased from the Acrylonitrile Plant of the Chemical Department of Mailiao Formative Plastics Company. The concentrated hydrochloric acid was purchased from Guangdong Guanghua chemical factory co., ltd. *N*-pentane was purchased from Tianjin Damao Chemical Reagent Factory. All reagents were used as received without further purification.

3.1. Materials Synthesis. PBO gels were prepared by the acid-catalyzed preparation method proposed by Shruti.[20] The BO monomer was mixed with DMF. Then, the mixed solution was stirred thoroughly at about 80 °C until it is fully dissolved, and the hybrid solution was held to cool down to room temperature. Hydrochloric acid was mixed with DMF, and then, the mixture was mixed with BO monomer solution and stirred at room temperature for 15 min. After that, the mixture was transferred to the mold, gelled for 3 h at 50 °C, then molded, followed by solvent exchange. The order of solvents is nitrogen dimethyl amide, acetone, acetonitrile, and *n*-pentane. Each solvent is used twice for 12 h each time. Low-polarity solvents can reduce solvent volatilization during subsequent atmospheric drying, which would result in the destruction of the pore structure by the capillary force in the micropores of the wet gel, thus preventing the pore structure of aerogels from being destroyed as far as possible. After that, the wet gel is placed at room temperature and atmospheric pressure for a day and then subjected to subsequent heat treatment at a specific temperature. To explore the influence of the T_c on the performance of PBO aerogel, a set of different T_c (room temperature, 120, 150, 180, 200 °C) were imposed for comparison.

https://doi.org/10.1021/acsomega.2c01300
ACS Omega 2022, 7, 26116−26122

4. RESULTS AND DISCUSSION

The PBO wet gel prepared by acid catalysis is yellowish-green and turns brown and solid after heat treatment, as shown in Figure 1b. The ring-opening polymerization reaction that

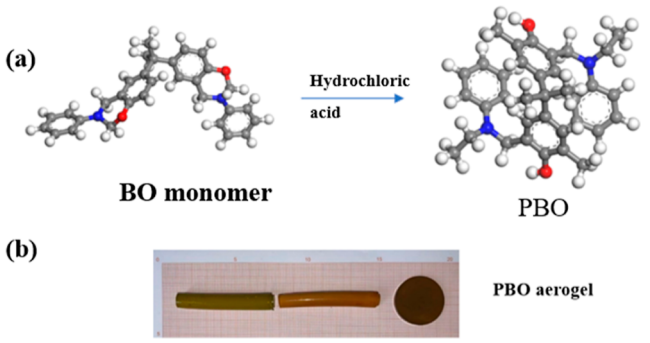

Figure 1. (a) General mode of polymerization of the BO monomer. (b) PBO before (left) and after (right) heat treatment.

occurred in the acid-catalyzed cross-linking and curing process was further understood by the infrared spectrum shown in Figure 2a. The strong absorption peak of the BO monomer at 690^{-1}, which is attributed to the true stretching vibration of the C−H bond outside the aniline plane, disappeared utterly. The cyclic acetal/amino stretching of the BO monomer at 939 cm^{-1} and the pH−O−C stretching at 1226 cm^{-1} were replaced by a new absorption peak near 1266 cm^{-1}, which was attributed to the phenolic C−O stretching. This also shows a strong −OH− rise at 3420 cm^{-1}, indicating extensive −OH− extension in the PBO aerogel. As T_c increases, −OH− of the PBO aerogel is stronger, implying that phenol forms −OH− due to the ring-opening of the BO monomer. During the curing reaction, the polymerization reaction further occurs, and the increase of T_c makes the polymerization reaction more sufficient. In addition, it can be seen from the infrared spectrum that the strong asymmetric/symmetric −C−O−C− stretching (1228 and 1031 cm^{-1}) and the stretching of cyclic acetals have significantly weakened or disappeared with curing treatment. As can be seen in Figure 2a, the disappearance of the peak at 1442 cm^{-1}, which is attributed to the char−char stretching in the substituted benzene torus, further indicated that the PB monomer had completed ring-opening polymerization to form PBO aerogel. The absorption peak at 2991 cm^{-1} is mainly attributed to the stretching of −C−H−, while the absorption peak at 1300 to 1700 cm^{-1} is primarily due to the extension of C═C in the benzene ring. For other absorption peaks, there are firm absorption peaks at 747 and 690 cm^{-1}, which are attributed to the bending vibration of the −C−H− bond hanging on the surface of the aromatic ring and the monomers in aniline, and these peaks also begin to weaken slightly with the increase of temperature. As shown in Figure 2b, we tested the structure of PBO aerogels, and there is a wide peak at 21.8° and no crystallization peak, so it is speculated that the polymer has the amorphous structure.

Figure 3a reveals the significant effects of curing treatment on the compressive properties of PBO aerogel. When T_c is 120 °C, Young's modulus and the toughness of PBO aerogel are the lowest; with increasing T_c, Young's modulus, toughness, and compressive strength of the aerogel increased gradually. This was because PBO aerogel, a kind of thermosetting phenolic resin increasing the curing temperature to a certain range, was beneficial to the further cross-linking curing of the BO monomer. The robustness of the overall cross-linked skeleton structure gradually increases with the increase of T_c. Therefore, their mechanical properties such as ultimate strain and stress, compressive strength, and Young's modulus of PBO aerogel gradually increased with T_c in the range of 120−200 °C.

Compared with the PBO aerogels reported in other literature, the mechanical properties of aerogels prepared in this study increase significantly, as shown in Figure 3b. When the bulk density ρ_b is 0.46 g/cm^3, Young's modulus (E) of the PBO aerogel prepared in previous work[23] is about 223 MPa, which is higher than those of other high-performance aerogels of similar density, including polyimide and polyamide (Kevlar-like) aerogels, as well as polymer-cross-linked X-silica and X-vanadia aerogels. In contrast, the value of E reaches 733 MPa for the as-prepared PBO aerogel sample in this study at a similar density (0.48 g/cm^3). The value of E for PBO aerogel prepared by Shruti[20] is about 490 MPa when ρ_b is 0.55 g/cm^3, while for the as-prepared PBO aerogel, E reaches 831 MPa when ρ_b is 0.53 g/cm^3. Young's modulus of aerogel prepared in this study is much higher than that of others. Specifically, when the post-treatment temperature reached 200 °C, Young's modulus of PBO aerogel reached a maximum of 1070.11 ± 11.21 MPa, which is even higher than other previously reported values.[23−25]

Figure 4 shows the thermogravimetric (TG) and (b) DTG curves of PBO aerogel prepared at different T_c. The PBO aerogel obtained at atmospheric pressure, that is, without post-treatment, has the lowest thermal stability and final residual char (≈43%). With the increased T_c, the thermal stability of

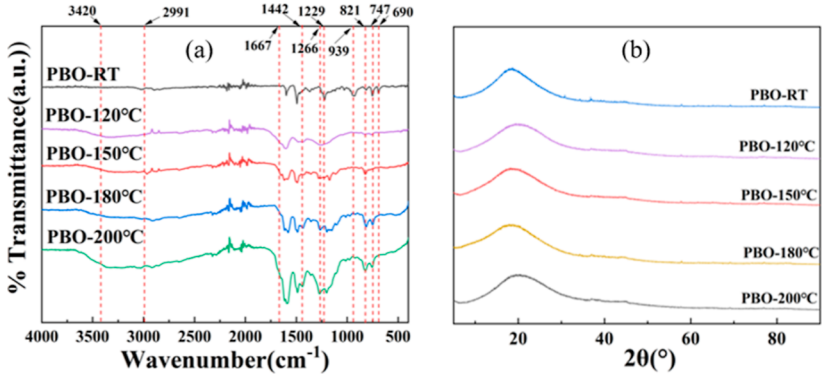

Figure 2. (a) Infrared spectra of benzoxazine aerogel at the different curing temperatures. (b) XRD spectrum.

https://doi.org/10.1021/acsomega.2c01300
ACS Omega 2022, 7, 26116−26122

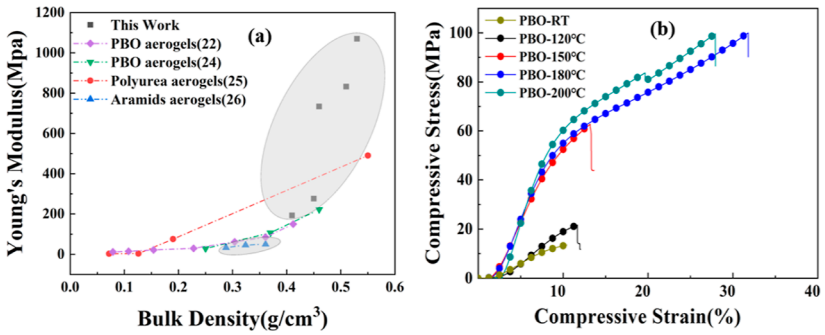

Figure 3. (a) Stress−strain curves of PBO aerogels at different curing temperatures. (b) Comparison of Young's modulus with that of aerogels in other literature.

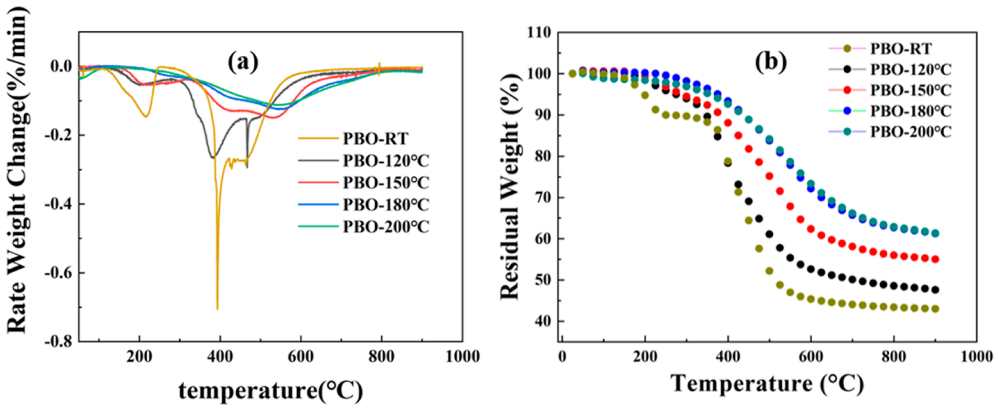

Figure 4. (a) DTG and (b) TG curves of the as-prepared PBO aerogels at different treatment temperatures.

Table 1. Mechanical Property Parameters of PBO Aerogels Obtained at Different Curing Temperatures and Aerogels in Other Literatures

name	ultimate strain (%)	ultimate stress (MPa)	Young's modulus (MPa)	compressive stress (MPa)
PBO-RT	13.21	10.01	193.32 ± 4.61	5.94 ± 0.21
PBO-120	21.03	11.24	275.81 ± 5.14	5.76 ± 0.38
PBO-150	60.73	12.50	733.76 ± 8.65	22.78 ± 4.38
PBO-180	98.84	31.34	832.32 ± 9.34	23.85 ± 2.47
PBO-200	98.61	27.51	1070.11 ± 11.21	24.62 ± 1.80
PBO aerogel[21]			150.12	
PBO aerogel[23]			222.3	
aramid aerogel[25]			50.24	
polyurea aerogel[24]			490.45	
lignin/graphene oxide aerogel[29]				2.188 ± 0.21
polyurethane aerogels[30]			1.2	0.04

PBO aerogel increases gradually and reached the peak when the subsequent T_c was about 180 °C, where the temperature at 10% mass loss was 438 °C, and the char residual rate at 800 °C was 63 wt %. Comparatively, for PBO aerogels prepared by Lorjai, the temperature of 10% mass loss was 425 °C, and the char residual rate at 800 °C was 53 wt %.[14] The char residual rate at 800 °C for PBO aerogels prepared by Shruti was 53−61 wt %.[20] Therefore, it is clear that the prepared F-type PBO aerogels have certain advantages in thermal stability and residual char rate. The influence of T_c on thermal stability and the final residual char rate is related to the secondary cross-linking of aerogels at different T_c. As thermosetting resin, the cross-linking reaction of BO at high T_c makes the skeleton structure of aerogel more robust, resulting in higher strength and higher thermal stability. Polybenzoxazine aerogel begins to decompose at high temperature, and the primary decomposition products of bisphenol-A/aniline-based polybenzoxazine are a combination of benzene derivatives, amines, phenolic compounds, Schiff base compounds, and Mannich base compounds.[32]

To clarify the origin of superior mechanical and thermal stability, the porous structure of the PBO aerogels was studied through N_2-sorption measurements at all curing temperatures. Quantitatively, the open pore volume and the average pore diameter of the aerogels were also calculated (Tables 1 and 2). Similar to our previous studies,[23] no signs of microporosity can be found in N2-sorption isotherms, which indicates that the PBO aerogels are partly mesoporous and mainly macroporous materials. The hysteresis loops become wider and reach shorter saturation plateaus at higher T_c, which means that the mesoporous portion of the materials at higher T_c is more significant than that at lower temperatures. However, the trend

https://doi.org/10.1021/acsomega.2c01300
ACS Omega 2022, 7, 26116−26122

Table 2. Pore Structure of PBO Aerogel Obtained at Different Curing Temperatures

name	BET surface area, σ (m^2 g^{-1})	$V_{1.7-300nm}$	average pore diameter (nm)	
			4 V/σ	BJH method
PBO-RT	77.12	0.38	10.41	20.82
PBO-120 °C	50.19	0.15	7.26	13.41
PBO-150 °C	37.73	0.10	6.37	12.31
PBO-180 °C	67.02	0.34	11.04	22.64
PBO-200 °C	56.21	0.13	6.50	12.01

reverses when the curing temperature exceeds 180 °C, where the micropores can be destroyed or merged into macropores.

To further understand the microstructure of PBO, SEM images of the aerogel samples are shown in Figures 5 and 6. The porous structure of stacked-up particles with diameters between 10 and 100 nm can be identified for samples prepared without curing treatment. In the range from room temperature to 180 °C, the particle diameter of aerogels increases markedly at elevated T_c, the links between the particles also become sturdier, leading to structural transformation from pearl necklace to the worm. Besides, the random secondary particle aggregation is also enhanced. These changes create a more stable and robust three-dimensional disordered porous network with promoted mechanical properties. On the other hand, if the curing temperature is too high, sintering phenomena will occur between aerogel particles, like what happened in samples PBO-200, as shown in Figure 6, where the original spherical particles begin to agglomerate, resulting in the sharp decrease of the pore volume and specific surface area, just consistent with that observed in the BET test.

It can be seen from the data in Table 3 that the curing temperature exposes a significant effect on the thermal properties of PBO aerogel. For samples obtained without curing treatment, the thermal conductivity is 0.122 W/m·k. With increasing T_c, λ continues decreasing to a minimal value of 0.086 W/m·k at 180 °C and turns to increase after that point. When the curing temperature reaches 200 °C, the value of λ even becomes more prominent than that of PBO, which did not undergo subsequent curing treatment.

In porous aerogels, a large number of pores with dimensions smaller than the diffusion-free path of air molecules can restrict the movement of air molecules, to effectively reduce the intensity of convective heat transfer; in contrast, the aerogel network structure prolongs the distance required for solid-phase heat transfer, so aerogels possess extreme low thermal conductivity, even lower than that of air. When the curing temperature reaches 200 °C, the volume of pores in PBO aerogels decreases significantly, and the intensity of convective heat transfer is strengthened. Moreover, the increase of the density, caused by elevated T_c, leads to a further reduction in the heat transfer distance of the solid phase. Therefore, thermal conductivity of aerogels increases, as shown in Figure 7. Compared with other aerogels, the thermal conductivity of the as-prepared aerogels is close or even lower.

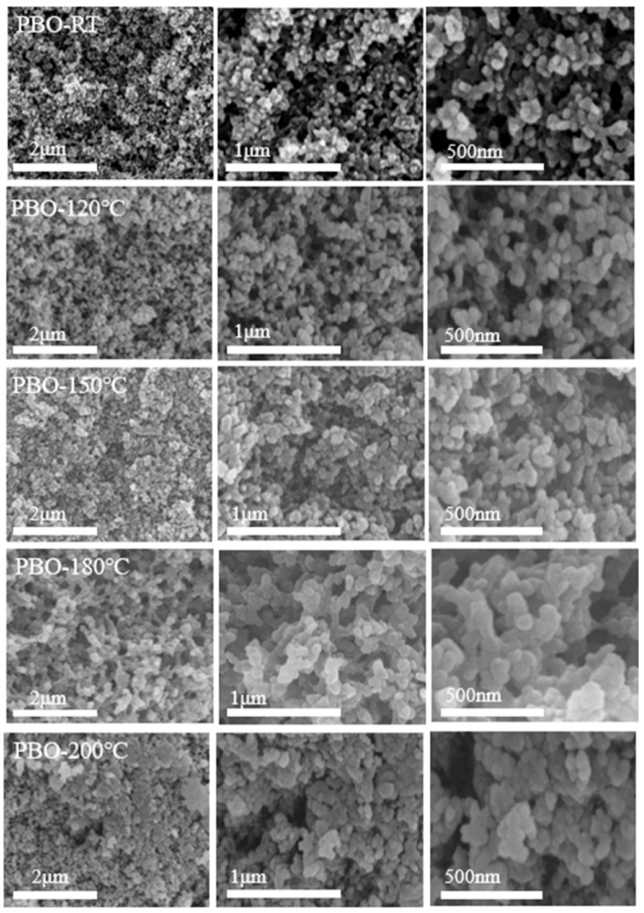

Figure 6. SEM image of PBO aerogel at different treatment temperatures.

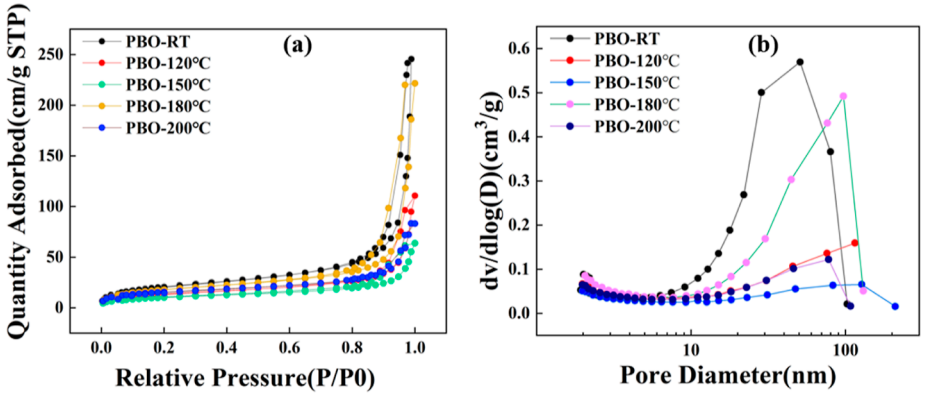

Figure 5. (a) N_2 sorption measurements of the PBO aerogels: isotherm and (b) BJH plots.

https://doi.org/10.1021/acsomega.2c01300
ACS Omega 2022, 7, 26116−26122

Table 3. Bulk Density, Thermal Resistance, and Thermal Conductivity of PBO Aerogels

name	bulk density, ρ_b (g/cm^3)	thermal resistance, R (m^{2}k/w)	thermal conductivity, λ (W/m·k)
PBO-RT	0.465	0.0246	0.122
PBO-120 °C	0.476	0.0624	0.099
PBO-150 °C	0.483	0.0782	0.091
PBO-180 °C	0.531	0.0831	0.086
PBO-200 °C	0.572	0.0326	0.138
PBO aerogel[20]	0.38		0.069
PBO aerogels[21]	0.913		0.037
polybenzoxazine aerogels[23]	0.262		0.097
porous aramids aerogels[25]	0.913		0.913
SiO_2 aerogel[26]	0.126		0.031
SiO_2 aerogel[27]	0.217		0.027
polyurethane aerogels[30]	0.18		0.017
silica-polyurethane aerogel[31]	0.58		0.066

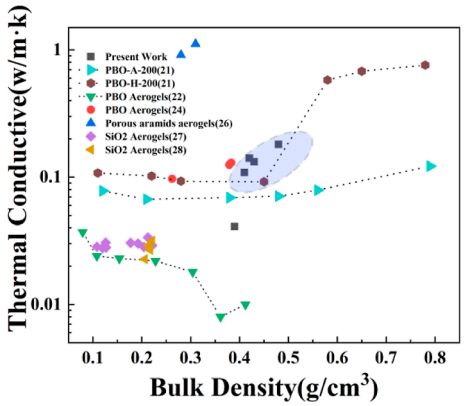

Figure 7. Thermal conductivity of PBO and porous aramid aerogels at different densities.

In addition to the above properties, the flame-retardant properties of the prepared aerogels were also measured. It was found that this aerogel extinguished itself instantly despite exposure to the alcohol lamp (≈660 °C), like that reported by Xiong.[28] All these excellent properties enable the aerogels prepared to be used in aerospace and other fields.

5. CONCLUSIONS

The F-type polybenzoxazine aerogels with high strength, excellent thermal stability, and low thermal conductivity were successfully prepared by the acid-catalyzed polymerization of bisphenol F benzoxazine. The effects of different treatment temperatures on the properties of benzoxazine aerogels were studied by setting different treatment temperatures. Finally, the optimal treatment temperature of bisphenol A-type PBO aerogel prepared by us is 180 °C. At this heat treatment temperature, Young's modulus of benzoxazine aerogel is as high as 831 MPa (0.53 g/cm^3), which is much higher than that of other aerogels with the same density, and the residual char rate reaches 62%, so that it can be used as the precursor of char aerogel. The thermal conductivity is 0.086 W/mK.

AUTHOR INFORMATION

Corresponding Author

Guanglei Zhang − *School of Materials Science and Engineering, Shijiazhuang Tiedao University, Shijiazhuang 050043, China; Hebei Provincial Engineering Research Center of Metamaterials and Micro-device, Shijiazhuang 050043, China*; Phone: +8631187936084; Email: zhgl@stdu.edu.cn; Fax: +8631187935416

Authors

Guoqiang Qin − *School of Materials Science and Engineering, Shijiazhuang Tiedao University, Shijiazhuang 050043, China; Hebei Provincial Engineering Research Center of Metamaterials and Micro-device, Shijiazhuang 050043, China*

Shilun Jiang − *School of Materials Science and Engineering, Shijiazhuang Tiedao University, Shijiazhuang 050043, China; Hebei Provincial Engineering Research Center of Metamaterials and Micro-device, Shijiazhuang 050043, China*; orcid.org/0000-0002-3270-3013

Haotian Zhang − *School of Materials Science and Engineering, Shijiazhuang Tiedao University, Shijiazhuang 050043, China; Hebei Provincial Engineering Research Center of Metamaterials and Micro-device, Shijiazhuang 050043, China*

Shengjian Qin − *School of Materials Science and Engineering, Shijiazhuang Tiedao University, Shijiazhuang 050043, China; Hebei Provincial Engineering Research Center of Metamaterials and Micro-device, Shijiazhuang 050043, China*

Hongya Wu − *School of Materials Science and Engineering, Shijiazhuang Tiedao University, Shijiazhuang 050043, China; Hebei Provincial Engineering Research Center of Metamaterials and Micro-device, Shijiazhuang 050043, China*

Feipeng Zhang − *Institute of Sciences, Henan University of Urban Construction, Pingdingshan 467036, P. R.China*

Complete contact information is available at: https://pubs.acs.org/10.1021/acsomega.2c01300

Notes

The authors declare no competing financial interest.

ACKNOWLEDGMENTS

This work was funded by the Natural Science Foundation of China under grant no. 51502179, Hebei Natural Science Foundation under grant no. E2020210076 and Foundation of Hebei Educational Committee under grant no BJ2021037.

REFERENCES

(1) Baskakov, S. A.; Baskakova, Y. V.; Kabachkov, E. N.; Dremova, N. N.; Michtchenko, A.; Shulga, Y. M. Novel Superhydrophobic Aerogel on the Base of Polytetrafluoroethylene. *ACS Appl. Mater. Interfaces* **2019**, *11*, 32517−32522.

(2) Karamikamkar, S.; Fashandi, M.; Naguib, H. E.; Park, C. B. In Situ Interface Design in Graphene-Embedded Polymeric Silica Aerogel with Organic/Inorganic Hybridization. *ACS Appl. Mater. Interfaces* **2020**, *12*, 26635−26648.

(3) Kistler, S. S. Coherent Expanded Aerogels and Jellies. *Nature* **1931**, *127*, 741.

(4) Tian, T.; Hou, J.; Ansari, H.; Xiong, Y.; L'Hermitte, L.; Danaci, D.; Pini, R.; Petit, C. Mechanically stable structured porous boron nitride with high volumetric adsorption capacity. *J. Mater. Chem. A* **2021**, *9*, 13366−13373.

(5) Zhang, S.; Feng, J.; Feng, J.; Jiang, Y. Formation of enhanced gelatum using ethanol/water binary medium for fabricating chitosan aerogels with high specific surface area. *Chem. Eng. J.* **2017**, *309*, 700−707.
(6) Lee, B. H.; Yoon, B.; Abdulagatov, A. I.; Hall, R. A.; George, S. M. Growth and Properties of Hybrid Organic-Inorganic Metalcone Films Using Molecular Layer Deposition Techniques. *Adv. Funct. Mater.* **2013**, *235*, 532−546.
(7) Zhang, K.; Yu, X. Catalyst-free and low-temperature terpolymerization in a single-component benzoxazine resin containing both norbornene and acetylene functionalities. *Macromolecules* **2018**, *51*, 6524−6533.
(8) Xiao, Y.; Li, L.; Zhang, S.; Feng, J.; Jiang, Y.; Feng, J. Thermal insulation characteristics of polybenzoxazine aerogels. *Macromol. Mater. Eng.* **2019**, *304*, 1900137.
(9) Xiao, Y.; Li, L.; Liu, F.; Zhang, S.; Feng, J.; Jiang, Y.; Feng, J. Compressible, flame-resistant and thermally insulating fiber-reinforced polybenzoxazine aerogel composites. *Materials* **2020**, *13*, 2809.
(10) Zhang, K.; Liu, Y.; Han, L.; Wang, J.; Ishida, H. Synthesis and thermally induced structural transformation of phthalimide and nitrile-functionalized benzoxazine: toward smart ortho -benzoxazine chemistry for low flammability thermosets. *RSC Adv.* **2019**, *9*, 1526−1535.
(11) Ohashi, S.; Iguchi, D.; Heyl, T. R.; Froimowicz, P.; Ishida, H. Quantitative studies on the p-substituent effect of the phenolic component on the polymerization of benzoxazines. *Polym. Chem.* **2018**, *9*, 4194−4204.
(12) Dumas, L.; Bonnaud, L.; Dubois, P. Polybenzoxazine Nanocomposites. *Advanced and Emerging Polybenzoxazine Science and Technology*; Elsevier Science, 2017; pp 767−800.
(13) Alhwaige, A. A.; Ishida, H.; Qutubuddin, S. Chitosan/polybenzoxazine/clay mixed matrix composite aerogels: preparation, physical properties, and water absorbency. *Appl. Clay Sci.* **2020**, *184*, 105403.
(14) Li, L.; Xiao, Y.; Zhang, S.; Feng, J.; Jiang, Y.; Feng, J. Lightweight, strong and thermally insulating polymethylsilsesquioxane-polybenzoxazine aerogels by ambient pressure drying. *J. Sol. Gel Sci. Technol.* **2021**, 1−10.
(15) Malakooti, S.; Qin, G.; Mandal, C.; Sotiriou-Leventis, C.; Leventis, N.; Lu, H. High Thermo-Mechanical Stability in Polybenzoxazine Aerogels//ASME International Mechanical Engineering Congress and Exposition. *Am. Soc. Mech. Eng.* **2019**, *59490*, V012T10A053.
(16) Xiong, S.; Yang, Y.; Zhang, S.; Xiao, Y.; Ji, H.; Yang, Z.; Ding, F. Nanoporous polybenzoxazine aerogels for thermally insulating and self-extinguishing materials in aerospace applications. *ACS Appl. Nano Mater.* **2021**, *4*, 7280−7288.
(17) Tiwari, I.; Sharma, P.; Nebhani, L. Polybenzoxazine-an enticing precursor for engineering heteroatom-doped porous carbon materials with applications beyond energy, environment and catalysis. *Mater. Today Chem.* **2022**, *23*, 100734.
(18) Zhang, S.; Sun, H.; Lan, T.; Xue, X.; Liu, X. Polybenzoxazine/boron nitride foam: a promising low-k, flame-retardant and robust material. *J. Mater. Sci.* **2021**, *56*, 18749−18761.
(19) Feng, Z.; Zeng, M.; Meng, D.; Zhu, W.; Liu, Y.; Huang, X. Novel recoverable porous magnetic carbons derived from biobased polybenzoxazine by self-foaming and activation treatment. *Colloids Surf., A* **2020**, *591*, 124559.
(20) Mahadik-Khanolkar, S.-K.; Donthula, S.; Sotiriou-Leventis, C.; Leventis, N. Polybenzoxazine aerogels. 1. High-yield room-temperature acid-catalyzed synthesis of robust monoliths, oxidative aromatization, and conversion to microporous chars. *Chem. Mater.* **2014**, *26*, 1303−1317.
(21) Xiao, Y.; Li, L.; Zhang, S.; Feng, J.; Jiang, Y.; Feng, J. Thermally insulating polybenzoxazine aerogels based on 4, 4′-diamino-diphenylmethane benzoxazine. *J. Mater. Sci.* **2019**, *54*, 12951−12961.
(22) Xiao, Y.; Li, L.; Zhang, S.; Feng, J.; Jiang, Y.; Feng, J. Thermal insulation characteristics of polybenzoxazine aerogels. *Macromol. Mater. Eng.* **2019**, *304*, 1900137.
(23) Malakooti, S.; Qin, G.; Mandal, H.; Soni, R.; Taghvaee, T.; Ren, Y.; Chen, H.; Tsao, N.; Shiao, J.; Kulkarni, S. S.; Sotiriou-Leventis, C.; Leventis, N.; Lu, H. Low-Cost, Ambient Dried, Superhydrophobic, High Strength, Thermally Insulating and Thermally Resilient Polybenzoxazine Aerogels. *ACS Appl. Polym. Mater.* **2019**, *1*, 2322−2333.
(24) Leventis, N.; Sotiriou-Leventis, C.; Chandrasekaran, N.; Mulik, S.; Larimore, Z. J.; Lu, H.; Churu, G.; Mang, J. T. Mang; Multifunctional Polyurea Aerogels from Isocyanates and Water. A StructureProperty Case Study. *Chem. Mater.* **2010**, *22*, 6692−6710.
(25) Leventis, N.; Chidambareswarapattar, C.; Mohite, D. P.; Larimore, Z. J.; Lu, H. Multifunctional porous aramids (aerogels) by efficient reaction of carboxylic acids and isocyanates. *J. Mater. Chem. A* **2011**, *21*, 11981−11986.
(26) Chen, F.; Zhang, Y.; Liu, J.; Wang, X.; Chu, P. K.; Chu, B.; Zhang, N. Fly ash-based lightweight wall materials incorporating expanded perlite/SiO_2 aerogel composite: Towards low thermal conductivity. *Constr. Build. Mater.* **2020**, *249*, 118728.
(27) Cai, H.; Jiang, Y.; Feng, J.; Zhang, S.; Peng, F.; Xiao, Y.; Li, L.; Feng, J. Preparation of silica aerogels with high temperature resistance and low thermal conductivity by monodispersed silica sol. *Mater. Des.* **2020**, *191*, 108640.
(28) Xiong, S.; Yang, Y.; Zhang, S.; Xiao, Y.; Ji, H.; Yang, Z.; Ding, F. Nanoporous Polybenzoxazine Aerogels for Thermally Insulating and Self-Extinguishing Materials in Aerospace Applications. *ACS Appl. Nano Mater* **2021**, *4*, 7280−7288.
(29) Yue, Y.; Wang, Y.; Li, Y.; Cheng, W.; Han, G.; Lu, T.; Huang, C.; Wu, Q.; Jiang, J. High strength and ultralight lignin-mediated fire-resistant aerogel for repeated oil/water separation. *Carbon* **2022**, *193*, 285−297.
(30) Diascorn, N.; Calas, S.; Sallée, H.; Achard, P.; Rigacci, A. Polyurethane aerogels synthesis for thermal insulation−textural, thermal and mechanical properties. *J. Supercrit. Fluids* **2015**, *106*, 76−84.
(31) Cho, J.; Jang, H. G.; Kim, S.Y.; Yang, B. Flexible and coatable insulating silica aerogel/polyurethane composites via soft segment control. *Compos. Sci. Technol.* **2019**, *171*, 244−251.
(32) Lorjai, P.; Wongkasemjit, S.; Chaisuwan, T.; Jamieson, A. M. Significant enhancement of thermal stability in the non-oxidative thermal degradation of bisphenol-A/aniline based polybenzoxazine aerogel. *Polym. Degrad. Stab.* **2011**, *96*, 708−718.

https://doi.org/10.1021/acsomega.2c01300
ACS Omega 2022, 7, 26116−26122